

ChemComm

Accepted Manuscript



This is an *Accepted Manuscript*, which has been through the Royal Society of Chemistry peer review process and has been accepted for publication.

Accepted Manuscripts are published online shortly after acceptance, before technical editing, formatting and proof reading. Using this free service, authors can make their results available to the community, in citable form, before we publish the edited article. We will replace this *Accepted Manuscript* with the edited and formatted *Advance Article* as soon as it is available.

You can find more information about *Accepted Manuscripts* in the [Information for Authors](#).

Please note that technical editing may introduce minor changes to the text and/or graphics, which may alter content. The journal's standard [Terms & Conditions](#) and the [Ethical guidelines](#) still apply. In no event shall the Royal Society of Chemistry be held responsible for any errors or omissions in this *Accepted Manuscript* or any consequences arising from the use of any information it contains.



Journal Name

COMMUNICATION

Dual template effect of Supercritical CO₂ in Ionic Liquid to Fabricate Highly Mesoporous Cobalt Metal-Organic Framework

Received 00th January 20xx,
Accepted 00th January 20xx

Huanan Yu, Dongdong Xu, Qun Xu*

DOI: 10.1039/x0xx00000x

www.rsc.org/

Hierarchical meso- and microporous metal-organic framework (MOF) was facilely fabricated in an ionic liquid (IL)/supercritical CO₂ (SC CO₂)/surfactant emulsion system. Notably, CO₂ plays a dual effect during the synthesis, that is, CO₂ droplets were utilized as template for the cores of nanospheres while CO₂-swollen micelles induce mesopores on nanospheres.

As a new class of porous crystalline materials with diverse fascinating topologies and permanent porosity after desolvation, metal-organic frameworks (MOFs) have emerged as an attractive material for a remarkably wide range of potential applications, including gas separation, drug delivery, catalysis, and energy storage.¹⁻³ Nowadays, much effort has been devoted to the use of MOFs as energy materials.^{4,5} Compared with conventional carbon materials, MOFs are a new type of electrode material for their intrinsic pseudo-capacitive redox centers.⁶ However, most of the porous MOFs adopt microporous regime (<2 nm), which largely restrict the diffusion and mass transfer as electrode materials.^{7,8} Therefore, researchers have continuously focused on designing nanoscale MOFs with hierarchical meso- and micropores for their advantages of providing dispersion of active sites at various length scales of pores.⁹

In recent years, ionic liquids (ILs) and supercritical CO₂ (SC CO₂), known as unconventional and green solvents, have received a lot of attention in the synthesis of new materials.¹⁰ ILs can be designed to satisfy various requirements of the applications owing to their excellent solvency for both inorganic and organic compounds, high chemical and thermal stability, negligible vapor pressures, wide electrochemical windows and liquid temperature range.¹¹ SC CO₂, which is also an interesting class of solvent with advantages of low toxicity, low cost and nonflammability, has been widely used in different fields as reaction media and material processing. More importantly, the chemical and physical properties of SC CO₂ can be tuned easily by varying operating temperature and pressure.^{12,13}

Traditionally, amphiphilic surfactants can be utilized to synthesize various interesting materials with controlled micro-morphologies such as micelles, vesicles, liquid crystals, etc.^{14,15} When the fabrication process is realized in CO₂ or ILs, it will bring us new possibilities.¹⁶ In particular, the fluorinated surfactants have an excellent CO₂-responsive ability to dissolve much CO₂ in micelles and the amount of dissolved CO₂ can be easily tuned by changing CO₂ pressure.¹⁷ To date, the formation of mesoporous materials with assistance of IL or SC CO₂ is very attractive due to their unusual solvent properties.¹⁸ Zhang et al. reported that mesoporous polymers with tunable thin mesopore walls and large mesopores were synthesized through a CO₂-swollen micelle templating route. Du et al. studied the fabrication of mesoporous silica nanospheres by using a trisiloxane-tailed ionic liquid as a template.²⁰ Fabricating hierarchically meso- and microporous materials and further tuning their porous structure efficiently is an interesting work, however, still a big challenge.

In this work, we devised a reaction system to help build surfactant-directed assembly of porous structure in a switchable solution, in which it contains surfactant, ionic liquid and SC CO₂. For this system, it has bi-function, one is creating dispersed phase of microemulsions containing SC CO₂, and the other is formation of continuous phase of ionic liquid. Here we choose Co-MOF as the research object, so a series of Co-MOF with large BET surface area and high mesoporosities are formed. Specifically, the Co-MOF is made up of a microporous framework stemming from organic ligand bridged by Co²⁺, and numerous mesopores in nanospheres construct the molecular sieve-like structure. Moreover, the interconnected worm-like structure constructs a series of macropores to further enrich the hierarchical porosity of Co-MOF. During the synthesis of nanospheres, CO₂ takes on dual function. One hand, CO₂ droplets dispersed in IL can be utilized as template to help form the cores of nanospheres; on the other hand, the CO₂-swollen micelles will induce numerous mesopores on the shell of nanospheres. Both the size and mesopore properties of nanospheres can be easily tuned by changing CO₂ pressure. Significantly, the as-synthesized hierarchically meso- and microporous Co-MOF can be tested as electrode material, which exhibits a high specific capacitance of 230.5 F g⁻¹ at 0.5 A g⁻¹.

^a College of Material Science and Engineering, Zhengzhou University, Zhengzhou

^b 450001, P. R. China. E-mail: qunxu@zzu.edu.cn.

Electronic Supplementary Information (ESI) available: [details of any supplementary information available should be included here]. See

DOI: 10.1039/x0xx00000x

COMMUNICATION

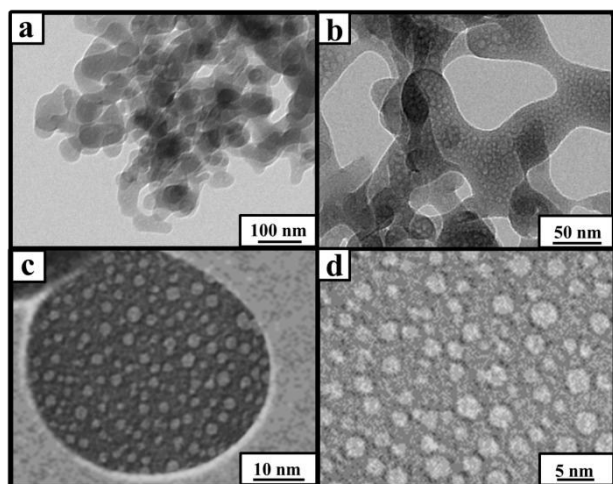


Fig. 1 TEM images (a-d) of the Co-MOF synthesized in an IL/SC CO₂/surfactant emulsion system at 16 MPa and 80 °C for 48 h.

The morphology and microstructure of samples were examined by SEM and TEM. As shown in Fig. 1a, the Co-MOF synthesized at 16 MPa for 48 h were uniform nanospheres with diameter of about 50 nm. These connective nanospheres with plenty of pores construct a worm-like morphology in Fig. 1b. Moreover, the interconnected worm-like structure construct a series of macropores to further enrich the hierarchical porosity of Co-MOF (Fig. S1b). Fig. 1c and d clearly shows numerous mesopores on nanospheres, which is similar to the structure of molecular sieve. The pore size and wall thickness were about 3 and 2 nm, respectively. When we shorten the reaction time to 24 h, nanospheres with smaller size appear a serious conglutination (Fig. S2).

Thermogravimetric analysis curve (Fig. S3a) shows the first part of weight loss was 7.3 wt%, which is mainly from the removal of absorbed H₂O and ethanol. Then, the Co-MOF is stable up to about 275 °C. In general, an obvious weight loss of 41.2 wt% is observed from 275 to 445 °C, which is likely corresponding to the thermal decomposition of Co-MOF crystallites. Fourier transform infrared spectra (Fig. S3b) revealed that the ligand KHBDC (Potassium acid phthalate) has two major absorption bands of protonated BDC at about 1566 cm⁻¹ and 1290 cm⁻¹. In sharp contrast, the Co-MOF shows the strong characteristic absorption for the asymmetric and symmetric vibration of BDC at about 1523 cm⁻¹ and 1335 cm⁻¹. The wavenumber difference of asymmetric and symmetric vibration of BDC anions for Co-MOF is narrowed. This indicates that both carboxylate groups of the BDC are coordinated to Co^{II} ions.²¹ Besides, the characteristic CH₃ stretching vibration (2962-1872 cm⁻¹) and C-N stretching vibration (1230-1030 cm⁻¹) for both IL and surfactant in Co-MOF were not observed, demonstrating that the product is free of N-EtFOSA and TMGA. It means that they could be easily removed by degassing and washing with ethanol. The wide-angle powder X-ray diffraction pattern (Fig. S3c) presents several sharp peaks, which is consistent with the reported Co-MOF,²² indicating that the synthesized Co-MOF is well-crystalline. Based on both EDX spectrum and XPS analysis in Fig. S4, Co, O and C components are found in Co-MOF.

The porosity properties of the Co-MOF were determined by N₂ adsorption-desorption method after the sample was dried at 60 °C. Fig. 2a shows a typical type IV isotherm and exhibits the pore

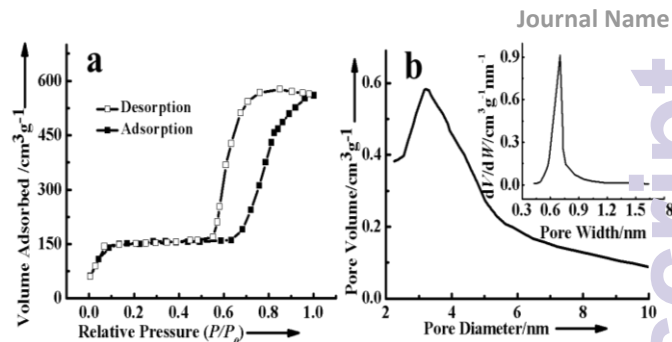


Fig. 2 N₂ adsorption-desorption isotherm (a) and mesopore size distribution curve (b) of Co-MOF synthesized in an IL/SC CO₂/surfactant emulsion system. The inset in (b) shows the micropore size distribution curve.

condensation with pronounced adsorption-desorption hysteresis, indicating that plenty of mesopores exist in the Co-MOF. The BET surface area, the total specific pore volume and mesopore volume are 720 m² g⁻¹, 0.49 cm³ g⁻¹ and 0.131 cm³ g⁻¹, respectively. The mesopore size distribution curve in Fig. 2b shows a pore distribution centered around 3.2 nm, which is obtained from Barrett-Joyner-Halenda method. This data is consistent with that measured from the TEM images shown in Fig. 1c and d. Furthermore, the Co-MOF has a high N₂ adsorption capacity when P/P_0 (the relative pressure) is as low as 0.01, indicating that mesoporous Co-MOF synthesized owns micropores structure. By using the Horvath-Kawazoe analysis, the micropore size was calculated to be 0.71 nm (inset in Fig. 2b) and the surface area of micropores is 426 m² g⁻¹ ($S_{\text{meso}}/S_{\text{micro}} = 0.51$). The analysis above confirms that hierarchical meso-micro porous structure of Co-MOF was formed and as well as the mesopores walls are constructed from a microporous framework.

To explore the formation process of mesoporous Co-MOF in the IL/SC CO₂/surfactant emulsion system, we prepared a series of contrast tests. As shown in Fig. S5a and b, the pink Co-MOF in the absence of IL but with SC CO₂ has a lot of mesopores. However, the single flaky structure shows no more multilevel pores. When prepared in IL without SC CO₂, the product also appears single flaky structure but without mesopores, and the color turns white (Fig. S5c and d), indicating that the reaction nearly cannot happen under this condition. Only in the presence of both IL and SC CO₂, mesoporous Co-MOF nanospheres were successfully fabricated (Fig. S5e and f). The reaction mechanism can be suggested as Fig. 3.

First, in the absence of CO₂, surfactant molecules self-assemble into cylindrical micelles through the hydrogen bonding interaction between the NH group of N-EtFOSA and IL atoms. The fluorinated tails of surfactant point to the inner, while the hydrophilic head groups arrange towards the continuous IL phase, forming the “dry” micelles with the empty cores. Second, SC CO₂ dissolves in the IL and enters into the micellar core to form a CO₂-swollen micelle. At the same time, CO₂ droplets are dispersed in the IL continuous phase with the aid of CO₂-swollen cylindrical micelles of the surfactant. Third, owing to the facile linkage property of Co²⁺ and BDC, the Co^{II} metal ions react with the deprotonated BDC in the IL phase to form a crystalline microporous framework, which leaves the cavities in micelles. At last, hierarchically meso- and microporous Co-MOFs were formed after the removal of CO₂, IL and surfactant by degassing and washing with ethanol. During the

synthesis of nanospheres, CO₂ plays dual template role. One hand, CO₂ droplets were dispersed in IL to help form the cores of nanospheres. On the other hand, these CO₂-swollen cylindrical micelles act as a template for the formation of mesopores on the shell of nanospheres. This differs a lot from the manuscript, in which Zhao et al. reported the micelles' orderly self-assembly induced the formation of well-ordered mesopores.²¹ In this work, it needs to address the effect of SC CO₂. Because of the good solvency of IL, the viscosity of reaction system can be reduced effectively by the CO₂ expansion. Thus this reaction for MOF formation between the metal salt and organic linker could be accelerated, which is reflected from the different color of the product. So it could be concluded that the coexistence of IL and SC CO₂ favors the formation of the mesoporous framework.

The Co-MOF with various pore structures was further synthesized in an IL/SC CO₂/surfactant system at different CO₂ pressure. Both N₂ adsorption-desorption isotherms in Fig. S7 exhibit an intermediate mode between type I and type IV, which are related to mesopores and micropores, respectively. The experimental results show that all Co-MOFs present hierarchically meso- and microporous structures. From 8 to 16 MPa, the average diameter of nanospheres increases from 18 to 50 nm (Fig. S6), while the mesopore diameter reduces from 6 to 3 nm (Table S1). Notably, the higher pressure favors the formation of larger nanospheres and smaller mesopores. According to the proposed mechanism above, this phenomenon can be explained as follows. At higher pressure, the surfactant is more CO₂ soluble, thus the interface becomes less curved about CO₂ and the size of CO₂ droplet is increased.²³ Therefore, the nanospheres synthesized at higher pressure have larger size because of the template effect of CO₂ droplets. As for the reduced mesopore size of the Co-MOF made at higher CO₂ pressure, it can be attributed to the decreasing amount of CO₂ solubilized in the micelles, a phenomenon which has been reported for CO₂-in-water micelles and CO₂-in-IL micelles.²⁴ The results indicate that both the size and mesopore properties of nanospheres can be easily tuned by controlling the CO₂ pressure.

The unique structure of the Co-MOF inspired us to evaluate its electrochemical performance for supercapacitor. As shown in Fig.

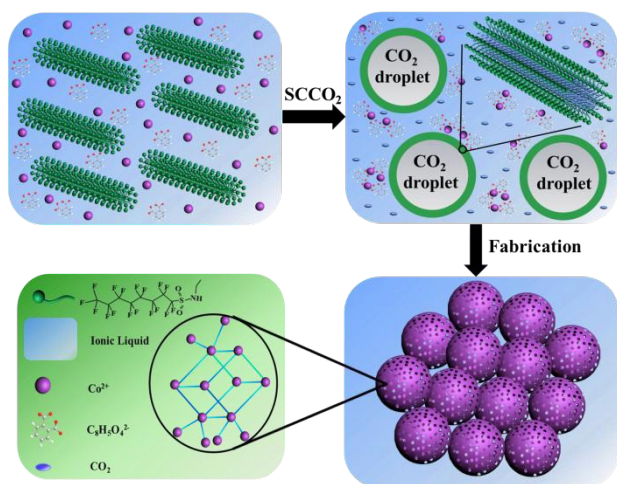


Fig. 3 Schematic illustration for the formation of mesoporous Co-MOF in an IL/SC CO₂/surfactant emulsion system.

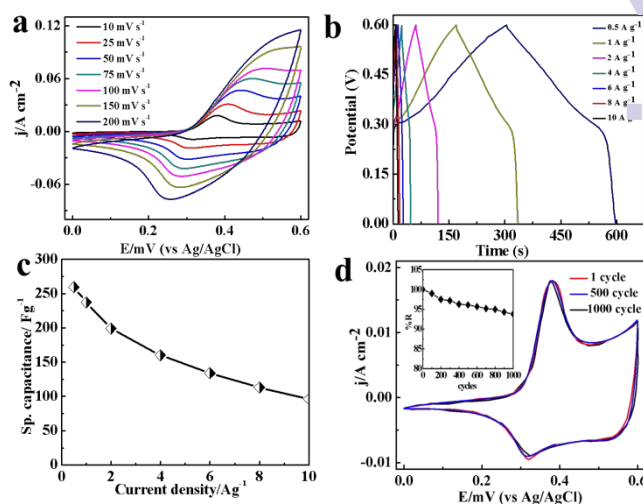


Fig. 4 (a) CV curves of the Co-MOF electrode at different scan rates. (b) Galvanostatic charge-discharge profiles at different current densities. (c) Specific capacitances of the Co-MOF electrode at different current densities. (d) Cycling stability of Co-MOF at a current density of 2 A g⁻¹ and the corresponding CV curves at a scan rate of 10 mV s⁻¹.

4a, the representative CV curves show a pair of well-defined redox peaks, suggesting that the demonstrated capacitive property is controlled by pseudocapacitance, rather than the appositely charged electrical double layer. The appearance of nearly symmetric potential-time curves in Fig. 4b indicates that the unique electrode has a low polarization and high charge-discharge columbic efficiency. Fig. 4c shows the porous Co-MOF exhibits the highest specific capacitance of 230.5 F g⁻¹ at 0.5 A g⁻¹, which is almost two times capacitance of cobalt oxides.^{25,26} This outstanding electrochemical performance should come from the novel structure of Co-MOF. First, the unique molecular sieve-like structure with high porosity increases the amount of electroactive sites, facilitating the transport of electrolyte and boost the electrical conductivity. Furthermore, the worm-like structure link to each other and serve as ion reservoirs, which accelerate the process of ion diffusion by diminishing the diffusion distance to the interior surfaces, so as to enhance the electrochemical property (Fig. S8). The long-term cycling performance of Co-MOF electrode was measured by galvanostatic charge-discharge tests for 1000 cycles (Fig. 4d). From the corresponding CV curves, the electrochemical redox switching is reversible perfectly for a long run. The specific capacitances of Co-MOF still retain 95.2% in capacitance after 1000 cycles, indicating that the as-prepared Co-MOF not only represents a high capacitance, but also an excellent stability when used as electrode material.

In summary, Co-MOF with novel hierarchical meso-micro pores was simply fabricated by the dual template function of SC CO₂ in IL. Both the size and mesopore properties of nanospheres can be easily tuned by changing CO₂ pressure. By taking advantages of interconnected nature of the hierarchically porous nanosphere, the Co-MOF exhibits a high specific capacitance of 230.5 F g⁻¹ at 0.5 A g⁻¹, which is the highest data ever reported for Co-MOFs. We believe that this simple and potentially universal design strategy

supplies a new way to fabricate more functional MOFs with novel morphologies and porosities in the near future.

We are grateful for the National Natural Science Foundation of China (No. 51173170, 50955010, and 20974102), the financial support from the Innovation Talents Award of Henan Province (114200510019), the Program for New Century Excellent Talents in University (NCET) and the Key program of science and technology (121PZDGG213) from Zhengzhou Bureau of science and technology.

Notes and references

- 1 N. Stock and S. Biswas, *Chem. Rev.*, 2011, **112**, 933.
- 2 F. Zheng, Y. Yang and Q. Chen, *Nat. Commun.*, 2014, **5**, 5261.
- 3 J. Cui, Y. Li, Z. Guo and H. Zheng, *Chem. Commun.*, 2013, **49**, 555.
- 4 D. Wu, Z. Guo, X. Yin, Q. Pang, B. Tu, L. Zhang and Q. Li, *Adv. Mater.*, 2014, **26**, 3258.
- 5 Y. Tan, W. Zhang, Y. Gao, J. Wu and B. Tang, *RSC Adv.*, 2015, **5**, 17601.
- 6 K. M. Choi, H. M. Jeong, J. H. Park, Y. B. Zhang, J. K. Kang and O. M. Yaghi, *ACS nano*, 2014, **8**, 7451.
- 7 H. Furukawa, N. Ko, Y. B. Go, N. Aratani, S. B. Choi, E. Choi and O. M. Yaghi, *Science*, 2010, **329**, 424.
- 8 K. Koh, A. G. Wong-Foy and A. J. Matzger, *Chem. Commun.*, 2009, **41**, 6162.
- 9 Y. Li, Z. Y. Fu and B. L. Su, *Adv. Funct. Mater.*, 2012, **22**, 4634.
- 10 J. Zhang and B. Han, *Acc. Chem. Res.*, 2012, **46**, 425.
- 11 M. V. Fedorov, and A. A. Kornyshev, *Chem. Rev.*, 2014, **114**, 2978.
- 12 P. G. Jessop and B. Subramaniam, *Chem. Rev.*, 2007, **107**, 2666.
- 13 A. P. Nelson, O. K. Farha, K. L. Mulfort and J. T. Hupp, *J. Am. Chem. Soc.*, 2008, **131**, 458.
- 14 S. H. Wu, C. Y. Mou and H. P. Lin, *Chem. Soc. Rev.*, 2013, **42**, 3862.
- 15 D. C. Shuai, J. Su, Q. Liu, Y. Jennifer, A. K. Gerasimov, W. Zajaczkowski and Herrmann, *Adv. Mater.*, 2015, **27**, 2459.
- 16 Y. Zhao, J. Zhang, B. Han, S. Hu and W. Li, *Green Chem.*, 2010, **12**, 452.
- 17 J. Liu, S. Cheng, J. Zhang, X. Feng, X. Fu and B. Han, *Angew. Chem. Int. Ed.*, 2007, **46**, 3313.
- 18 A. Chandran, K. Prakash and S. Senapati, *J. Am. Chem. Soc.*, 2010, **132**, 12511.
- 19 L. Peng, J. Zhang, S. Yang, B. Han, X. Sang, C. Liu and G. Yang, *Chem. Commun.*, 2014, **50**, 11957.
- 20 Z. Du, E. Li, G. Wang and F. Cheng, *RSC Adv.*, 2014, **4**, 4836.
- 21 Y. Zhao, J. Zhang, B. Han, J. Song, J. Li and Q. Wang, *Angew. Chem. Int. Ed.*, 2011, **50**, 636.
- 22 D. Y. Lee, D. V. Shinde, E-K. Kim, W. Lee, I-W. Oh, N. K. Shrestha, J. K. Lee and S. H. Han, *Microporous Mesoporous Mater.*, 2013, **171**, 53.
- 23 S. S. Adkins, X. Chen, I. Chan, E. Torino, Q. P. Nguyen, A. W. Sanders and K. P. Johnston, *Langmuir*, 2010, **26**, 5335.
- 24 L. Peng, J. Zhang, J. Li, B. Han, Z. Xue and G. Yang, *Angew. Chem. Int. Ed.*, 2013, **52**, 1792.
- 25 F. Meng, Z. Fang, Z. Li, W. Xu, M. Wang, Y. Liu and X. Guo, *J. Mater. Chem. A*, 2013, **1**, 7235.
- 26 J. Deng, L. Kang, G. Bai, Y. Li, P. Li, X. Liu and W. Liang, *Electrochim. Acta*, 2014, **132**, 127.